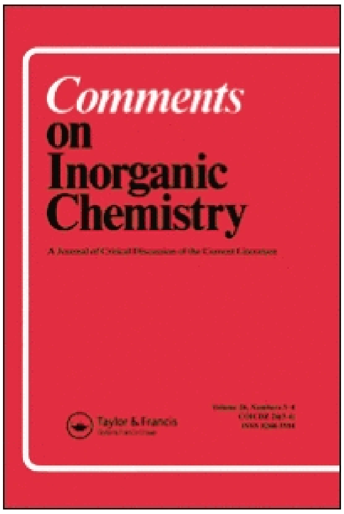

Comments on Inorganic Chemistry
Publication details, including instructions for authors and subscription information:
http://www.informaworld.com/smpp/title~content=t713455155

Vibrations of the Interstitial Atoms in Transition Metal Clusters

Pier Luigi Stanghellini[a]; Rosanna Rossetti[b]
[a] Dipartimento di Chimica, Università di Sassari, Sassari, Italy [b] Dipartimento di Chimica Inorganica, Chimica Fisica e Chimica dei Materiali, Università di Torino, Torino, Italy

To cite this Article Stanghellini, Pier Luigi and Rossetti, Rosanna(1990) 'Vibrations of the Interstitial Atoms in Transition Metal Clusters', Comments on Inorganic Chemistry, 9: 5, 263 — 303
To link to this Article: DOI: 10.1080/02603599008045478
URL: http://dx.doi.org/10.1080/02603599008045478

Vibrations of the Interstitial Atoms in Transition Metal Clusters

PIER LUIGI STANGHELLINI
*Dipartimento di Chimica,
Università di Sassari,
via Vienna 2,
I-07100 Sassari, Italy*

ROSANNA ROSSETTI
*Dipartimento di Chimica Inorganica,
Chimica Fisica e Chimica dei Materiali,
Università di Torino,
via Pietro Giuria 7, I-10125 Torino, Italy*

Key Words: *carbido, hydrido, interstitial, metal cluster, nitrido, vibrational spectroscopy*

INTRODUCTION

The interstitial metal clusters form a fascinating class of complexes of the transition metals, where a non-metallic atom X is uniquely bonded to the metal atoms of the core. From the structural point of view, two subclasses might be distinguished, the properly called "interstitial" clusters, where the heteroatom is completely surrounded by the metal atoms of the cage in which it is inserted, and the "semi-interstitial" or "exposed" clusters, where the heteroatom is placed on, or nearby, a face or an edge of a metal polihedron. Moreover, even if the carbon atom remains the first reported and the most commonly encountered heteroatom, one example at least has appeared with hydrogen[1], nitrogen,[2] boron,[3]

Comments Inorg. Chem.
1990, Vol. 9, No. 5, pp. 263–303
Reprints available directly from the publisher
Photocopying permitted by license only

phosphorous,[4] sulphur,[5] silicium,[6] arsenic[7] and antimony[8] interstitial atoms. Together with these more common systems, there is an increasing number of policarbido and polihydrido complexes, containing several interstitial heteroatoms[9]; recently, an example of a cluster with carbon and hydrogen together was reported.[10] Furthermore, some dicarbido clusters have a C_2 unit, with the two carbon atoms bonded to each other, in both interstitial[11] and exposed[12] configurations. Some selected examples of the core structures of interstitial (Fig. 1), exposed (Fig. 2) and poliheteroatom (Fig. 3) metal clusters are illustrated.

The first reported $Fe_5C(CO)_{15}$[13] appeared at that time to be no more than a structural curiosity, but in less than fifteen years the number of such complexes has grown so rapidly that they have assumed a central role in the metal cluster chemistry as far as concern the structural similarity with crystallites of the interstitial alloy, the reactivity of the heteroatom, the analogy with metal surface in which non-metallic atoms are embedded.

Even if research attention on this field has been mainly focussed on synthesis, structure and reactivity, an interesting topic is certainly the study of the vibrational properties of the interstitial

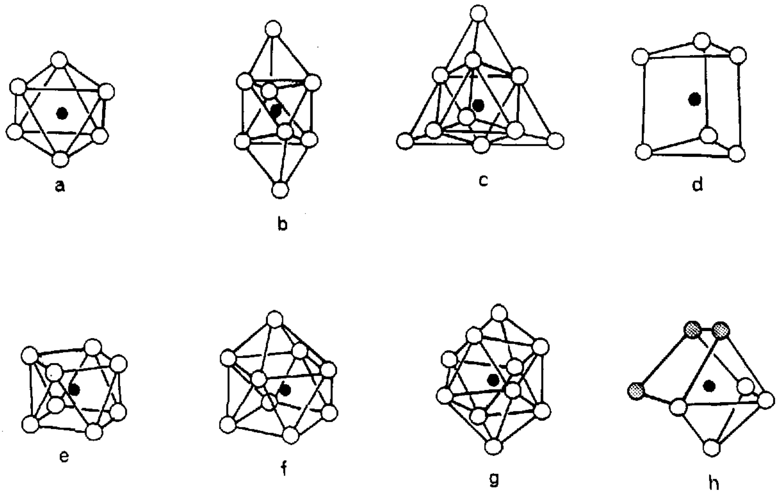

FIGURE 1 Selected examples of the core structures of interstitial metal carbonyl clusters: (a) $[Ru_6H(CO)_{18}]^-$; (b) $[Re_8C(CO)_{24}]^{2-}$; (c) $[Os_{10}C(CO)_{24}]^{2-}$; (d) $[Os_6P(CO)_{18}]^-$; (e) $[Ni_8C(CO)_{16}]^{2-}$; (f) $[Co_9Si(CO)_{21}]^{2-}$; (g) $[Rh_{10}S(CO)_{22}]^{2-}$; (h) $Fe_4B(CO)_{12}[AuP(C_6H_5)_3]_3$ (shaded circles Au atoms).

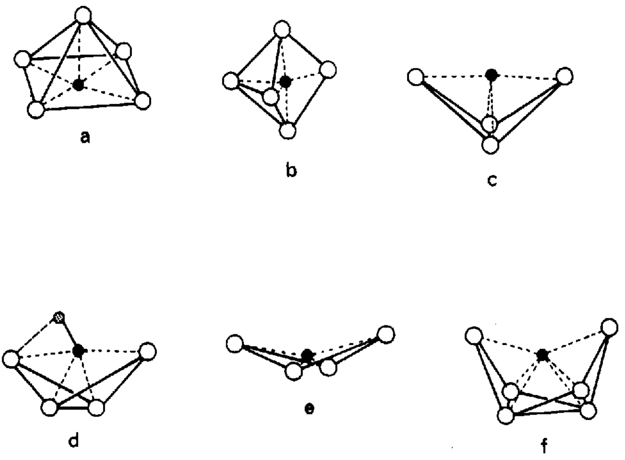

FIGURE 2 Selected examples of the core structures of exposed metal carbonyl clusters: (a) $Os_5C(CO)_{15}$; (b) $[Os_5C(CO)_{15}I]^-$; (c) $Fe_4C(CO)_{13}$; (d) $HFe(CH)(CO)_{12}$; (e) $[Re_4C(CO)_{15}I]^-$; (f) $[Co_6P(CO)_{16}]^-$.

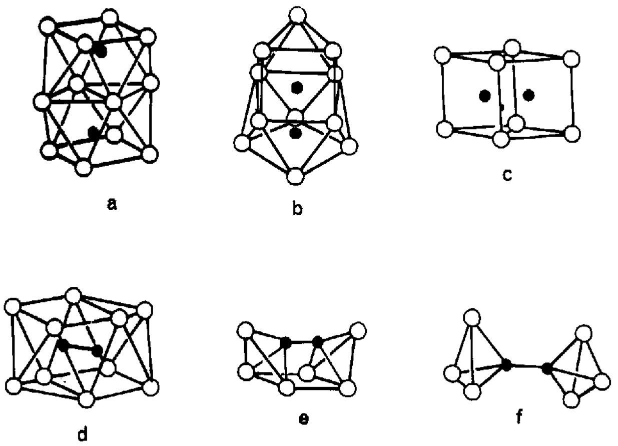

FIGURE 3 Selected examples of the core structures of interstitial and exposed dicarbido metal carbonyl clusters: (a) $[Rh_{12}(C)_2(CO)_{23}]^{4-}$; (b) $[Co_{11}(C)_2(CO)_{22}]^{3-}$; (c) $[Co_6Ni_2(C)_2(CO)_{16}]^{2-}$; (d) $[Ni_{10}C_2(CO)_{16}]^{2-}$; (e) $Co_6C_2(CO)_{14}S$; (f) $(CO)_9Co_3C_2Co_3(CO)_9$.

heteroatom, which in recent years are increasingly appearing, with the aim to explore the unusual metal–heteroatom bonding and the relationship with structural features. This forms the argument of this review, which has been divided into three main sections, concerning carbido, nitrido and hydrido metal clusters, the only groups where systematic vibrational studies were performed.

Systems like pyramidal (μ_3-X)M_3 traditionally are not regarded as exposed clusters, even if they formally might be, on the basis of the previous definition: anyway, we decided not to take them into account, except when X = C or H for completeness of information. Finally, no attention is given to the vibrational data not involving the encapsulated heteroatom, e.g., the ν(CO) features.

METAL CARBIDO CLUSTERS

The metal carbido clusters are the largest representative group of the interstitial compounds and their number is so rapidly growing that it has nearly doubled in two years, according to the lists reported in two subsequent reviews[14]: so it is not surprising that most of the vibrational data of the interstitial atoms are pertinent to the carbido carbon. In the first report on this topic the ν(M-C) modes were assigned to the bands observed at 790 and 770 cm^{-1} in the solution spectrum of the exposed carbido cluster $Fe_5C(CO)_{15}$. Some years later appeared the detailed assignment of the $Co_6C(CO)_{12}(\mu_3\text{-}S)_2$ (Fig. 4), unequivocally substantiated by the selected ^{13}C labeling.[15] From that time, it was clear that the vibrational modes of the interstitial or exposed carbido appear as medium-strong ir bands in the 900–500 cm^{-1} region. The corresponding Raman bands did not receive great attention, probably because the carbido clusters are poor Raman scatterers owing to their dark colors. Anyway, the ir bands alone are a useful and easily obtained analytical tool to infer the presence of an interstitial carbido atom in a newly prepared compound. The ^{13}C labeling is definitely convincing proof of the assignment and ought to be used in doubtful cases: incidentally, it offers information on the chemical origin of the interstitial atom.

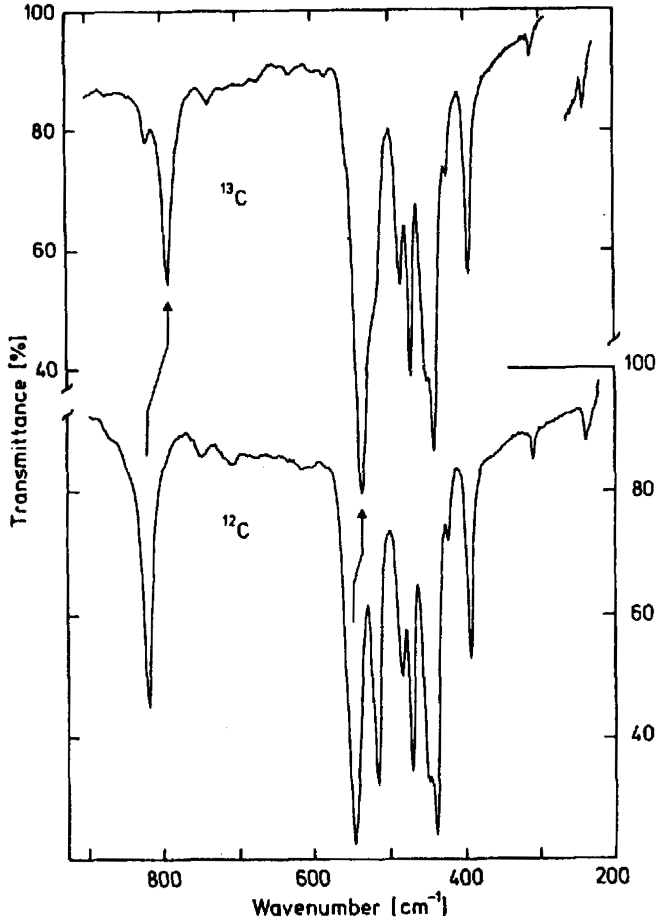

FIGURE 4 Ir spectra of $Co_6C(CO)_{12}S_2$ and its ^{13}C isotopomer in a KBr disk. (Corresponding to Fig. 3, p. 288 of G. Bor, U. K. Dietler, P. L. Stanghellini, G. Gervasio, R. Rossetti, G. Sbrignadello and G. A. Battiston, J. Organomet. Chem. **213**, 277 (1981).)

In this light, in several papers was assigned and discussed the carbido vibrational pattern. We have reported the vibrational data by classifying them on the basis of the carbido coordination and on the geometry of the metal cage: all the values are collected in Table I.

TABLE I

Values of the vibrational frequencies (cm^{-1}) of interstitial and exposed carbido atoms

Complex[a]	Symmetry[b]	ν(M-C)[c]	Assignment
$[Ru_6C(CO)_{16}][TMA]_2$	*d*	719	E
		690	A
$Ru_6C(CO)_{17}$	O_h	838	T_{1u}
$[Fe_6C(CO)_{16}][TMA]_2$	C_s	818	
		790	
		776	
$[Re_6C(CO)_{18}(\mu\text{-}H)_2][TEA]_2$	D_3	690	$A_2 + E$
$[Re_6C(CO)_{19}][TEA]^e_2$	C_1	678	
		660	
$[Re_8C(CO)_{24})[TEA]_2$	D_{3h}	696	E_u
		655	A_{2u}
$[Re_7AgC(CO)_{21}][TEA]_2$	C_{3v}	678	E
		635	A_1
$[Re_7C(CO)_{21}][TEA]_3$	C_{3v}	688	E
		662	A_1
$[Re_7C(CO)_{22}][TEA]$	C_s	695	A'
		685	A''
		670	A'
$[Os_{10}C(CO)_{24}][TMA]_2$	T_d	753	T_2
$(\mu\text{-}H)_2Os_{10}C(CO)_{24}$	*f*	773	
		760	
		735	
$Co_6C(CO)_{12}(\mu_3\text{-}S)_2$	D_{3h}	819	A''_2
		548	E'
$[Co_6C(CO)_{15}][PPN]_2$	D_{3h}	772	A''_2
		719	E'

$[Rh_6C(CO)_{15}][K]_2$	D_{3h}	689	A''_2
		653	E'
$[Ni_8C(CO)_{16}][TMA]_2$	D_{4d}	580	E
		524	B_2
$[Ni_9C(CO)_{17}][TMA]_2$	C_{4v}	582	E
		522	A_1
$[Ni_{10}C(CO)_{18}][TMA]_2$	g	584	E_1
$Fe_5C(CO)_{15}$[h]	C_{4v}	805	i
		775	
		766	
		790[j]	
		770[j]	
$Ru_5C(CO)_{15}$[c,k]	C_{4v}	757	i
		738	
		730	
$Os_5C(CO)_{15}$[c,k]	C_{4v}	793	i
		769	
		757	
$Ru_5C(CO)_{15}(\mu\text{-}H)Cl$	f	823	
		685	
$Ru_5C(CO)_{15}(\mu\text{-}H)Br$	f	823	
		687	
$Ru_5C(CO)_{14}P(C_6D_5)_3$[l]	C_s	741	A''
		701	A'
$Ru_5C(CO)_{14}(\mu\text{-}H)(\mu\text{-}SC_2H_5)$[l]	C_s	785	A''
		726	A'
$Ru_5C(CO)_{14}Br[\mu\text{-}AuP(C_6D_5)_3]$[l]	C_s	789	A''
		719	A'
$Ru_5C(CO)_{14}(\mu OCCH_3)[\mu\text{-}AuP(C_6H_5)_3]$[l]	C_s	800	A''
		717	A'
$Ru_5C(CO)_{15}(NCCH_3)$	C_{2v}	824	B_1
		685	B_2

TABLE I

(Continued)

Complex[a]	Symmetry[b]	ν(M-C)[c]	Assignment
		681	A_1
$Ru_5C(CO)_{15}Cl[\mu\text{-}AuP(C_6D_5)_3]$[e,l]	C_{2v}	835,825	B_1
		683,675	B_2
$Ru_5C(CO)_{15}(\mu\text{-}H)I$[l]	*f*	828	
		689	
$Ru_5C(CO)_{14}(\mu\text{-}H)I$[l]	*f*	777	
		733	
$Os_5C(CO)_{14}(\mu\text{-}H)(CO_2C_2H_5)$[l]	C_s	853	A''
		739	A'
$Os_5C(CO)_{14}(\mu\text{-}H)(C_5H_4N)$[l]	C_s	849	A''
		744	A'
$Os_5C(CO)_{16}$[e,l]		865	
		862	
		688	
		686	
$Os_5C(CO)_{14}I(CO_2CH_3)$[l]	*m*	898	A_2''
		641,613	E'
$[Fe_4C(CO)_{12}][PPN]_2$	C_{2v}	829	B_2
		666	A_1
		608	B_1
		272[n]	A_1^{o}
$[Fe_4C(CO)_{12}(\mu\text{-}H)][PPN]$	C_{2v}	922	B_2
		661	A_1
		609	B_1
		269[n]	A_1^{o}
$Fe_4C(CO)_{13}$	C_{2v}	928	B_2
		658	A_1

$Fe_4(CH)(\mu\text{-}H)(CO)_{12}$	C_s	252[n]	A_1^o
		824	A''
		657	A'
$[Fe_3RhC(CO)_{12}][PPN]$	C_s	248[n]	A'^o
		953	A''
		668	A'
$[Fe_3WC(CO)_{13}][PPN]_2$	C_s	274[n]	A'^o
		899	A''
		651	A'
$Co_6(C_2)(CO)_{14}(\mu_4\text{-}S)$	C_{2v}	263[n]	A'^o
		698[p]	B_1
		610[p]	A_1/B_2
$(CO)_9Co_3(C_2)Co_3(CO)_9$	D_{3d}	679[p]	
		661[p]	

[a] TMA = $[N(CH_3)_4]^+$; TEA = $[N(C_2H_5)_4]^+$; PPN = $N[P(C_6H_5)_3]_2^+$.

[b] Idealized symmetry of the metal core.

[c] Room temperature ir spectra in KBr or CsI disks, unless otherwise stated.

[d] Probably tetragonal or trigonal distorted octahedron.

[e] Presence of two crystallographic independent molecules in the unit cell.

[f] Structure not determined.

[g] Presumed D_{4d} structure.

[h] Two polimorphic crystalline forms.

[i] Assignment under discussion: see text.

[j] Ciclohexane spectrum.

[k] Complex spectrum at low temperature.

[l] Ir spectrum at 95°K.

[m] Presumed D_{3h} structure.

[n] Raman spectrum.

[o] Mainly Fe-Fe stretching.

[p] Motion of the rigid C_2 unit.

(1) Interstitial Clusters

(a) Octahedral cage

Five systems, having an idealized octahedral geometry of the M_6C core were reported. The $Ru_6C(CO)_{17}$ compound is interesting in that, whereas the geometry of the core is quite accurately octahedral, the overall symmetry including the CO groups is much lower, perhaps C_s.[16] The ir spectrum shows only a strong ν(Ru-C) band at 818 cm^{-1}, assigned to the T_{1u} mode[17] with the help of the ^{13}C labelling, indicating that the ν(M-C) band pattern is a reflection of the symmetry of the metal core and not of the molecular geometry. This was confirmed by the spectrum of $[Ru_6C(CO)_{16}]^{2-}$ which was reported to be distorted from the O_h symmetry without careful details[18] and by that of $[Fe_6C(CO)_{16}]^{2-}$, whose metal core itself has a C_s symmetry.[19] Two bands appeared in the former spectrum with intensity ratio ca. 2:1, leading to the prediction that the major distortion of the Ru_6 core is either trigonal or tetragonal; three bands appeared in the latter one, whose intensities are consistent with the 1:1:1 ratio, as expected by the core symmetry.

The two Re clusters have different geometry too, and different band patterns. The distortion of $[Re_6C(CO)_{18}(H)_2]^{2-}$ (D_3) from idealized octahedron is small[20] and the calculated splitting of the T_{1u} mode into A_2 and E modes is less than 1 cm^{-1}: accordingly, the spectrum exhibits a unique ν(Re-C) strong band.[21] $[Re_6C(CO)_{19}]^{2-}$ is completely unsymmetric; moreover, the unit cell contains two crystallographic independent molecules.[22] The broad ν(Re-C) band, which is splitted in two bands at low temperature, cannot be reasonably assigned.

(b) Capped octahedral cage

Several mono- and bi-capped octahedral rhenium carbido clusters have been reported, in which the symmetry of the metal core is lowered because of either the presence of the capping atoms or the distortion induced in the octahedral cage. The symmetry of the cores, $[Re_8C(CO)_{24}]^{2-}$ (D_{3h})[23], $[Re_7AgC(CO)_{21}]^{2-}$ (C_{3v}),[24] and $[Re_7C(CO)_{21}]^{3-}$ (C_{3v})[25] are such that the vibrational modes of the carbido atom give rise to two bands, one belonging to a degenerate, type E mode, and the other one to a non-degenerate, type A mode (Fig. 5). The intensity of the bands, the splitting effect at low

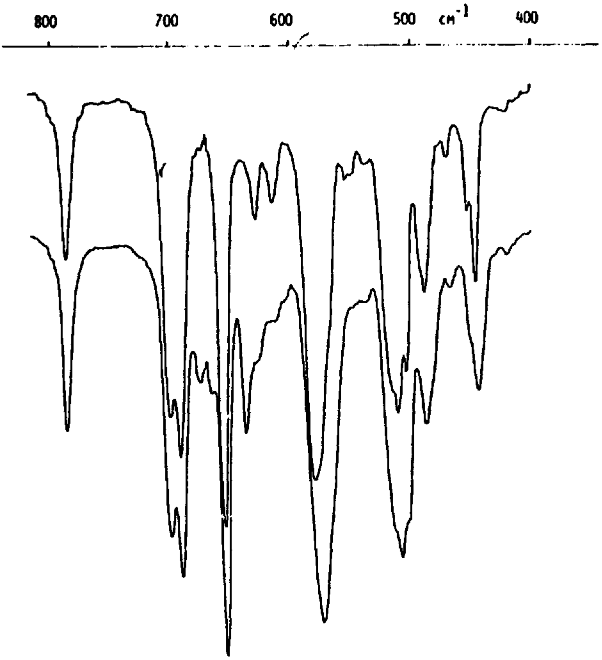

FIGURE 5 Ir spectra of $[Re_8C(CO)_{24}]^{2-}$ and its ^{13}C isotopomer in CsI disk. (Corresponding to Fig. 3, p. 2271 in P. L. Stanghellini, R. Rossetti, G. D'Alfonso and G. Longoni, Inorg. Chem. **26**, 2769 (1987).)

temperature and the ^{13}C isotope shift confirmed the assignment.[21] The distortion of the Re core due to one bridging CO lowers the symmetry of $[Re_7C(CO)_{22}]^-$ to C_s[22]: three ν(Re-C) modes are required and three bands appear in the spectrum at low temperature.

The structure of $[Os_{10}C(CO)_{24}]^{2-}$ consists of a tetracapped octahedral configuration of the Os_{10} core, with capping occurring on the alternate faces of the octahedron, so giving rise to an approximate T_d symmetry.[26] A single ν(Os-C) band is observed at room temperature, which splits at low temperature to a small extent. It was concluded that the immediate environment of the C atom is close to octahedron and that the difference of one octahedral axis from the other two could explain the small splitting at low temperature. The spectrum of the diprotonated species $H_2Os_{10}C(CO)_{24}$ shows three well resolved bands, which indicate the departure of the core structure from the pseudo-cubic symmetry and suggest that the protonation occurs in the central octahedral core.[27]

(c) *Trigonal prismatic cage*

The regular trigonal prism has D_{3h} symmetry, and, accordingly, the ν(M-C) span A_2'' and E' modes. Two bands appeared in the spectrum of $Co_6C(CO)_{12}(\mu_3\text{-}S)_2$[15], $[Co_6C(CO)_{15}]^{2-}$ and $[Rh_6C(CO)_{15}]^{2-}$ [28] and were correctly assigned on the basis of their relative intensities and of the ^{13}C isotope shifts. The high frequency band belongs to the A_2'' mode, the low frequency one to the E' mode, the separation being much larger in $Co_6C(CO)_{12}(\mu_3\text{-}S)_2$ than in the other two compounds, probably because of the large elongation of the prism along the z axis.

(d) *Square antiprismatic cage*

The carbido clusters with square antiprism structure are the only reported example where the coordination number around the carbido atom is greater than six. The structures are a square antiprism for $[Ni_8C(CO)_{16}]^{2-}$, a monocapped square antiprism for $[Ni_9C(CO)_{17}]^{2-}$ and, presumably, a bicapped square antiprism for $[Ni_{10}C(CO)_{18}]^{2-}$.[29] The symmetries, D_{4d}, C_{4v} and D_{4d}, respectively, require for the ν(Ni-C) vibrations one double degenerate E mode and one non-degenerate B_2 or A_1 mode. The two bands present in the spectra of all the compounds were readily assigned on the basis of intensity and isotope shift.[21] The ratio $\nu(A_1 \text{ or } B_2)/\nu(E)$ was easily calculated to be equal to h/l, when h is the height of the cage and l the side of the base. The good agreement between the two values related to the known complexes suggested the prediction that the $Ni_{10}C$ cage is a bicapped antiprism with flattened structure.

(2) Exposed Clusters

(a) *Five atom cage*

The three $M_5C(CO)_{15}$ (M = Fe, Ru, Os) compounds have basically the same structure, that is, a square pyramidal core of metal atoms in which the carbido atom is located ca. 0.1 Å below the center of the square base (Fig. 2). The idealized C_{4v} symmetry requires two M-C modes, A_1 and E representations, formally indicating the displacement of the C atom along the C_4 (z) axis and in the xy plane. They were assigned for the iron compound to the two bands at 805 cm^{-1} and at 766 cm^{-1}, respectively, owing to their intensity and shape, in particular the incipient splitting of the low energy band (Fig. 6).[30] More recent work, however, reported that $Fe_5C(CO)_{15}$ crystallizes in two polymorphic forms, which show slightly different ν(Fe-C) vibrations, namely at 805 and 765 cm^{-1}, and at 805 and 780 cm^{-1}, respectively, without any splitting: so the previous spectrum must be regarded as a superposition of the spectra of the two forms.[31] The analogous Ru and Os[30] carbido clusters give rise to ν(M-C) patterns similar to that of the Fe cluster, but at low temperature display greater complexity, with the appearance of two extra bands belonging to the M-C modes: the band multiplicity was explained by the presence of two unequivalent sets of molecules in the same unit cell.[32] The previous assignment of the ν(M-C) bands to A_1 and E modes was not in doubt until Powell and co-workers[33] reconsidered it on the basis of the correlation between metal-carbido stretching frequencies and cluster geometries in a series of Ru_5C clusters (see later). They suggested that the two M-C bands are the components of the splitted E mode, whereas the A_1 mode should have frequency below 600 cm^{-1}, so being covered by the strong δ(M-C-O) absorptions. This assignment is a consequence of an interesting spectra/structure relationship, but it does not appear completely convincing in that it requires very large shifts (30–40 cm^{-1}) between the E components, due to crystal structure effects, never observed for a degenerate metal-carbido stretching mode. Moreover, it does not explain the appearance of two bands in the $Fe_5C(CO)_{15}$ solution spectrum, where any structural deformation should be excluded. Anyway, this problem could be solved by getting information on band polarizability from the Raman spectra and on frequency shift from the spectra of the ^{13}C carbido labelled complexes.

The sensitivity of the metal-carbido stretching absorptions to the environment of the carbido atom has been confirmed by the aforementioned study on Ru_5C complexes. Starting from the 74 valence electrons $Ru_5C(CO)_{15}$ with close geometry, the addition of donor ligands gives rise to open clusters with arachno-pentagonal bipyr-

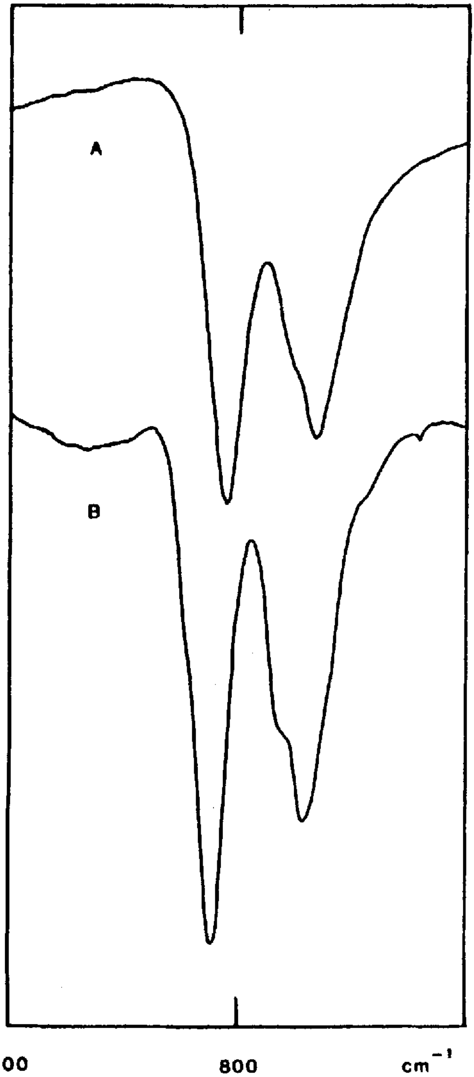

FIGURE 6 Ir spectra of $Fe_5C(CO)_{15}$ at 300 K (A) and 95 K (B) in a KBr disk. (Corresponding to Fig. 2, p. L260 in I. A. Oxton, D. B. Powell, R. J. Goudsmit, B. F. G. Johnson, J. Lewis, W. J. H. Nelson, J. N. Nicholls, M. J. Rosales, M. D. Vargas and K. H. Withmire, Inorg. Chim. Acta Lett. **64**, L259 (1982).)

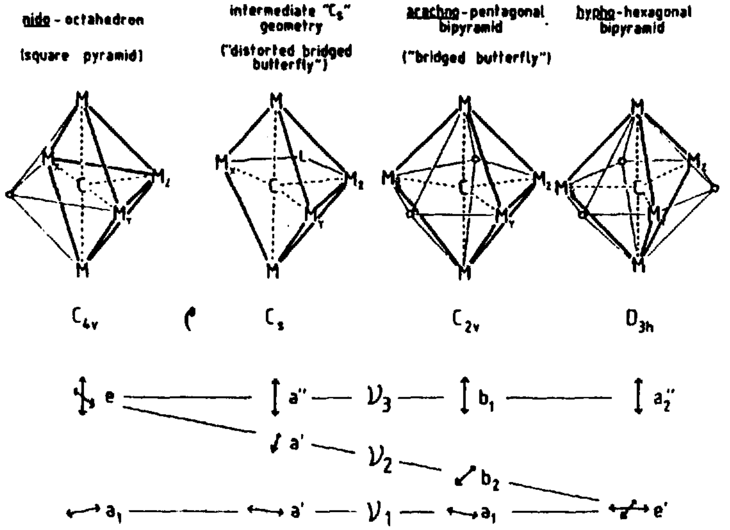

FIGURE 7 The metal-atom geometries of $[M_5C(CO)_{15}]$ (M = Ru, Os) clusters and their derivatives, showing the relationship between them. The approximate forms and symmetry correlations of the ν_{MC} modes are also depicted. (Corresponding to Fig. 1, p. 12 in C. E. Anson, D. B. Powell, A. G. Cowie, B. F. G. Johnson, J. Lewis, W. J. H. Nelson, J. N. Nicholls and D. A. Welch, J. Mol. Struct. **159**, 11 (1987).)

amidal (76 electrons) or hypho-hexagonal bipyramidal (78 electrons) geometries (Fig. 7). The M-C-M angle in the equatorial plane was taken as a measure of the extent to which the structure had opened up from the original geometry. When the angle decreases, the frequency separation between the two strong metal-carbido absorptions steadily increases: this relationship was used to predict the basic core structure of unknown Ru_5C clusters.[33]

(b) Four atom butterfly cage

The butterfly clusters with idealized C_{2v} symmetry $[Fe_4C(CO)_{12}]^{2-}$, $[HFe_4C(CO)_{12}]^-$ and $Fe_4C(CO)_{13}$ have four modes implying the motion of the semi-interstitial carbon atom (Fig. 8), but one of them, the $A_1(1)$ mode, involves very little motion of C because of the quasi-linearity of the Fe-C-Fe array. This mode gives rise to strong Raman band at ca. 260–280 cm^{-1}, easily assigned to A_1 because of its polarization in solution Raman spectrum. The three

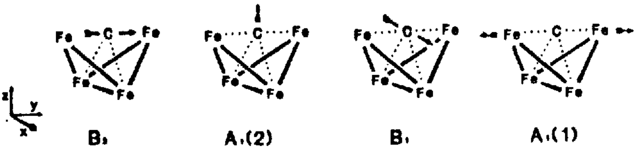

FIGURE 8 Schematic representations in approximate symmetry coordinates of the vibrational modes of the carbide atom in a butterfly cluster. The idealized symmetry is C_{2v}. (Corresponding to Fig. 1, p. 2951 in P. L. Stanghellini, M. J. Sailor, P. Kuznesof, K. H. Withmire, J. A. Hriljac, J. W. Kolis, Y. Zheng and D. F. Shriver, Inorg. Chem. **26**, 2950 (1987).)

other modes were assigned to the three medium-strong infrared bands whose frequencies are on the order $\nu(B_2) > \nu(A_1(2)) > \nu(B_1)$, on the basis of the ^{13}C labeling, with some uncertainty in the last mode which is partially covered by the strong δ(M-C-O) bands.[34]

Another group of butterfly carbides has C_s symmetry and includes the methyne cluster $HFe_4(CH)(CO)_{12}$ (Fig. 2) and the mixed-metal carbides $[Fe_3RhC(CO)_{12}]^-$ and $[Fe_3WC(CO)_{13}]^{2-}$ where the heteroatom occupies the hinge position in the cluster. The spectra of the carbides with C_s symmetry are qualitatively similar to those of the carbides with C_{2v} symmetry. The highest energy mode (A' for $HFe_4(CH)(CO)_{12}$, A'' for Fe_3M clusters, because of the different symmetry planes) and the A' mode, corresponding to $A_1(2)$ in C_{2v}, were easily discerned, together with the lowest frequency mode, observed in the Raman spectra in the 240–280 cm^{-1} region. It is noticeable that the high energy A' mode of $HFe_4(CH)(CO)_{12}$ has a frequency at 824 cm^{-1}, significantly lower than those of the other carbides, usually around 900 cm^{-1}. The nature of this vibration is such that it involves the motion of the carbon atom between the two wing-tip Fe atoms (Fig. 8): the agostic interaction of the CH group with one of the wing-tip Fe atoms lowers this Fe-C force constant significantly (see later).[34]

(3) Dicarbido Clusters

The literature reports only one example of the vibrational modes of a dicarbido C_2 unit: the complex, $Co_6C_2(CO)_{14}(\mu_4\text{-}S)$, is, at the same time, the only known example of exposed dicarbido cluster.

The structure (Fig. 3) shows a C_2 unit inserted in an open Co_6 "boat" framework with C-C axis parallel to the side of the boat base. The C_{2v} symmetry of the complex requires six "Co-C stretching" modes, $2A_1 + 2B_1 + A_2 + B_2$, all but A_2 infrared active. Two bands were considered to belong to vibrations of dominating ν(Co-C) character: one, at 698 cm^{-1}, was assigned to a B_1 mode in which an essentially rigid C_2 entity vibrates longitudinally relative to the boat. The other one, at 610 cm^{-1}, should be a B_2 mode or an A_1 mode (transversal or up-and-down vibrations of the C_2 unit with respect to the boat). Other modes were not assigned because of the overlap and the mixing with δ(Co-C-O) vibrations. Noteworthy is the C-C vibration of the dicarbido unit. assigned to a weak band ay 1444 cm^{-1}: the value is indicative of a bond order between one and two.[12]

By extending the definition of the exposed dicarbido clusters, the complex $(CO)_9Co_3C_2Co_3(CO)_9$ (Fig. 3) could be included, as the C_2 unit is bonded to the metal frame only.[35] Preliminary data on the C_2 vibrational modes were reported,[36] but the complete assignment is, at present, in progress.

METAL NITRIDO CLUSTERS

The metal nitrido clusters were recently reviewed[37] and appeared not to be of negligible number, even if much less than that of the carbido systems. Most of them belong to the exposed subclass, with the two most common geometries, the four-coordinated butterfly and the five-coordinated square pyramid; few systems have interstitial nitride, usually inserted in a hexametal cage.

The vibrational data associated with the nitrido atom are for examples of the most common interstitial and exposed systems: they are collected in Table II.

The two interstitial clusters, $[M_6N(CO)_{15}]^-$ (M = Co, Rh), have trigonal prismatic geometry, as do the aforementioned carbido systems. Two bands in the 600–750 cm^{-1} region, which are shifted by ^{15}N labelling, were easily assigned to the ν(M-N) modes. The treatment of the data was the same as that of the carbido clusters: the frequency order is $\nu(A''_2) > \nu(E')$.[28]

We wish to illustrate the yet unreported vibrational data on the

TABLE II

Values of the vibrational frequencies (cm^{-1}) of interstitial and exposed nitrido atoms

Complex[a]	Symmetry[b]	ν(M-N)[c]	Assignment
$[Co_6N(CO)_{15}][TPP]$[d]	D_{3h}	722	A_2''
		698	E'
$[Rh_6N(CO)_{15}][TPP]$[d]	D_{3h}	645	A_2''
		622	E'
$Fe_5N(CO)_{14}(\mu\text{-H})$	C_{4v}	936	E
		663	A_1
$Ru_4N(CO)_{12}(\mu\text{-H})$[e]	C_{2v}	863,856	B_2
		685	A_1^f
		623,621	B_1^f
$Ru_4N(CO)_{12}(\mu\text{-NCO})$	C_{2v}	863	B_2
		706	B_1
		595	A_1
$Ru_4N(CO)_{12}(\mu\text{-NO})$[e]	C_{2v}	863,859	B_2
		740,734	B_1
		591	A_1
$Ru_4N(CO)_{11}(\mu\text{-H})_3$	C_s	787	A''
		676	A'
		633	A'
$Os_4N(CO)_{12}(\mu\text{-H})$[e]	g	860,855,849	B_2
		733,722	B_1
		642,640,634	A_1

[a] TPP = $[P(C_6H_5)_4]^+$.

[b] Idealized symmetry of the metal core.

[c] Ir low temperature spectra in KBr disks, unless otherwise stated.

[d] Room temperature ir spectra in nujol.

[e] Presence of two crystallographic independent molecules in the unit cell.

[f] Reverse assignment: see text.

[g] Presumed C_{2v} structure with $\beta > 90°$.

$Fe_5(N)(\mu\text{-}H)(CO)_{14}$, as the unique example of pentanuclear nitrido exposed cluster.[38] Its core geometry is a roughly square pyramid with close Fe-Fe distances, despite the fact that three sides of the square base are bridged by CO groups and the fourth one by the hydrido atom (Fig. 9).[39] The idealized C_{4v} symmetry requires two modes, A_1 and E, for ν(Fe-N) stretching vibrations: the spectra, reported in Fig. 10, suggest the two strong absorptions at 936 and 663 cm^{-1} as the most probable candidates, the broad one at higher energy presumably belonging to the E mode, the other one to the A_1 mode, apparently mixed with bending modes of the bridging CO's. The low temperature spectrum also evidences the (Fe_2-μH) vibrations which we are inclined to assign to the bands at 1412 cm^{-1}(v_{asym}), 1338 cm^{-1} (v_{sym}) and 685 cm^{-1} (γ): the closeness of the symmetric and the asymmetric stretching frequencies suggests that the Fe-H-Fe angle has a value near 90°.[40]

Three medium-strong ir bands in the 600–900 cm^{-1} region were assigned to the ν(M-N) modes for the butterfly-shaped M_4N exposed nitrido clusters.[41] The approximate form of the symmetry coordinates for the idealized C_{2v} symmetry have been previously shown in Fig. 8 for the isostructural carbido complexes. The assignment to a specific mode was based on simple considerations of the cluster geometry, in particular the M_w-N and the M_h-N bond distances and the M_h-N-M_h (β) angle.[42] No doubt arises that the

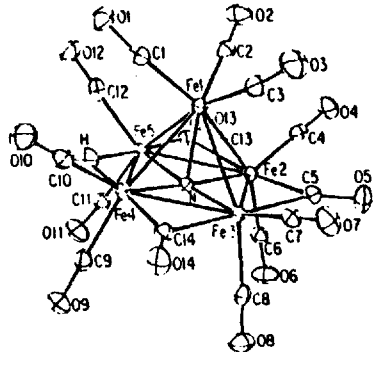

FIGURE 9 Molecular structure of $HFe_5N(CO)_{14}$. (Corresponding to Fig. 1, p. 6648 in M. Tachikawa, J. Stein, E. L. Muetterties, R. G. Teller, M. A. Beno, E. Gebert and J. M. Williams, J. Am. Chem. Soc. **102**, 6648 (1980).)

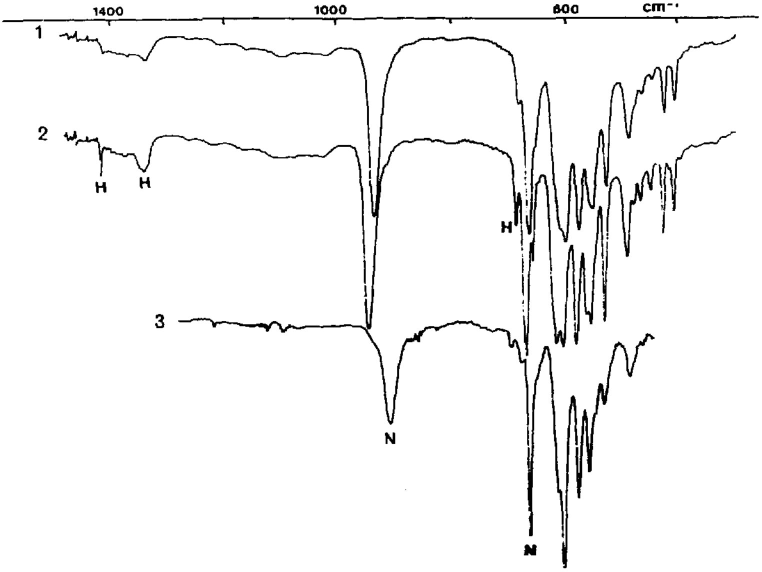

FIGURE 10 Ir spectra of $HFe_5N(CO)_{14}$ in a KBr disk at room temperature (1), at ca. 100 K (2) and in CS_2 solution (3) (N and H indicate the probable Fe-N and Fe-H stretching bands).

highest frequency band belongs to the B_2 mode,[43] because of the M-N distance values, M_w-N being shorter than M_h-N. The criterion used to assign the B_1 and $A_1(2)$ modes[44] was based on the change in frequency when the β angle value changes, arguing that as β increases, the frequency for the B_1 mode should increase and that for the A_1 mode should decrease. This qualitative argument has been substantiated by the vibrational analysis carried out on the isostructural carbido clusters, as $\nu^2(A_1)$ and $\nu^2(B_1)$ were calculated to be roughly proportional to $(1 + \cos\beta)$ and $(1 - \cos\beta)$, respectively.[34] Anyway, the frequency trends cannot avoid ambiguity of the assignment, which was resolved by observing that the predicted frequency order must be $\nu(B_1) > \nu(A_1)$ for $\beta > 90°$ and the reverse for $\beta < 90°$. In this light, the assignment reported in Table II has been interchanged with respect to that of Ref. 41 for $Ru_4N(CO)_{12}(\mu\text{-}H)$ and $Ru_4N(CO)_{11}(\mu\text{-}H)_3$ which have β less than 90°.[45]

The unequivocal assessment that the hydrogen atom is located in a metal cavity requires neutron diffraction analysis, which, in turn, requires large crystals to obtain suitable measurements. So the small number of systems where the presence of the interstitial hydrogen is unequivocally ascertained is not surprising; to our knowledge, they are at the moment the following ones: $[Co_6H(CO)_{15}]^-$,[1] $[Ru_6H(CO)_{18}]^-$,[46] Nb_6HI_{11},[47] $[Ni_{12}H(CO)_{21}]^{3-}$ and $[Ni_{12}(H)_2(CO)_{21}]^{2-}$,[48] which all lodge hydrogen in a more or less regular octahedral cavity.[49]

It is not an easy task to observe the infrared ν(M-H) bands of an interstitial hydrido cluster because of their inherent weakness and broadness. Substantial help can be obtained from the low temperature spectra where the bands considerably gain in sharpness and intensity and, of course, by the deuterium labelling of the interstitial hydride. Inelastic neutron scattering (INS) spectroscopy might improve the observations, because of its great sensitivity to the proton motion. There are considerable limits, however, like the scarce availability and the high cost of this technique, the poor resolution of the spectrum and the need for often unobtainable amounts of sample.

All the available frequency values are reported in Table III: the frequency unit is always cm^{-1}, even if the original data (INS spectra) are sometimes given in meV (conversion factor: 1 meV = 8.065 cm^{-1}).

The first report on the vibrations of interstitial hydrogen set an intriguing problem. The room temperature spectrum of the complex, $[Ru_6H(CO)_{18}]^-$, showed a broad doublet centered at ca. 825 cm^{-1}, doubtlessly assignable to the ν(Ru-H) modes, because of the shifting to ca. 600 cm^{-1} on deuteration.[51] On cooling, the absorptions became sharper and stronger, giving rise to two bands of almost equal integrated intensity (Fig. 11). The octahedral symmetry of the Ru_6 cage[46] should have given rise to a single band belonging to the triply degenerate T_{1u} mode. Moreover, any possible geometrical deformation or crystal site-group effect should have split the band into either two components (with 1:2 related intensity) or three components (with 1:1:1 related intensity). The D-complex spectrum did not offer unambiguous insight, as the

TABLE III

Values of the vibrational frequencies (cm^{-1}) of interstitial and exposed hydrido atoms

Complex[a]	Symmetry[b]	ν(M-H)[c]	Assignment
$[Ru_6H(CO)_{18}][TMA]$	O_h	825	T_{1u}
Nb_6HI_{11}	O_h	1090[d]	T_{1u}
$[Ni_{12}(H)_2(CO)_{21}][TMA]_2$	D_{3h}	667	$A_2'' + E'$
$[Ni_{12}H(CO)_{21}][TMA]_3$	C_{3v}	684	E
$[Co_6H(CO)_{15}][K]$	O_h	1086,1080[d]	T_{1u}
		960,949[d]	e
$[Co_6H(CO)_{15}][Cs]$	O_h	1080,1056[d]	T_{1u}
$Ru_6(\mu_3\text{-}H)_2(CO)_{18}$	D_{3d}	708	A_{2u}
		660,652	E_u
$[Os_6(\mu_3\text{-}H)(CO)_{18}][TBA]$	C_{3v}^{f}	1255	E
		1020	A_1
$Co_4(\mu_3\text{-}H)_4(\pi\text{-}C_5H_5)_4$	C_{3v}^{f}	1050	E
		958	A_1
$Co_3Fe(\mu_3\text{-}H)(CO)_{12}$	C_{3v}^{f}	1118	$A_1 + E$
$Co_3Ru(\mu_3\text{-}H)(CO)_{12}$	C_{3v}^{f}	1121	$A_1 + E$
$Co_3Os(\mu_3\text{-}H)(CO)_{12}$	C_{3v}^{f}	1109	$A_1 + E$

[a] TBA = $[N(nC_4H_9)_4]^+$.
[b] Idealized symmetry of the metal core.
[c] Low temperature ir spectrum in KBr or CsI disks, unless otherwise stated.
[d] Low temperature INS spectrum on solid sample.
[e] Assigned to the out-of-cage-hydrogen vibrations: see text.
[f] Idealized symmetry of the $(\mu_3\text{-}H)M_3$ unit.

ν(Ru-D) may or may not be a doublet (in the former case, the second component should be completely covered by the Ru-C-O absorptions: see Fig. 11). The final suggestion considered a component of the doublet as an overtone or a combination mode accidentally coupled with the ν(Ru-H) mode by Fermi resonance effect.

A broad peak centered at 135 meV, with small side absorptions, in the INS spectrum of Nb_6HI_{11} was assigned to the Nb-H stretching modes. The corresponding value for the deuterium compound appeared at 95 meV.[47] The side bands were probably due to impurities of β-niobium hydride, which can be formed during the synthesis of the cluster. The broadening of the main peak was attributed both to the low energy resolution of the spectrum (ca. 10%) and to the different Nb-H interactions due to the significant displacement of the H atom from the center of the cage.

A similar effect can explain the feature of the ir spectrum of $[Ni_{12}(H)_2(CO)_{21}]^{2-}$, where the hydrogen atoms are located in considerably distorted octahedral cavities and asymmetrically displaced from the center[48] (Fig. 12). A broad band centered at 678 cm^{-1} was considered a superposition of the bands generated by the splitting of the ν(Ni-H) T_{1u} mode, together with the coupling between the motions of the two hydrido atoms. In the other Ni cluster the H atom is so far from the center of the cavity as to be simply regarded as triply bridging to an Ni_3 triangle alone. Two

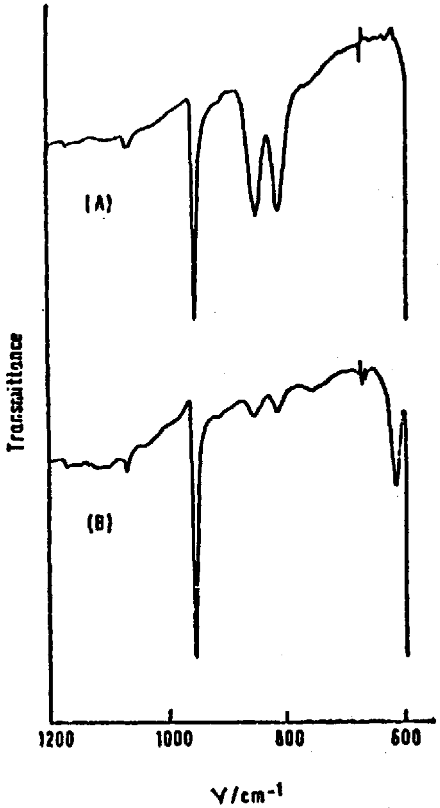

FIGURE 11 Ir spectra of $[Ru_6H(CO)_{18}]^-$ (A) and $[Ru_6D(CO)_{18}]^-$ (B) at 95 K in a KBr disk. (Corresponding to the figure on p. 688 in I. A. Oxton, S. F. A. Kettle, P. F. Jackson, B. F. G. Johnson and J. J. Lewis, Chem. Soc., Chem. Commun. 687 (1979).)

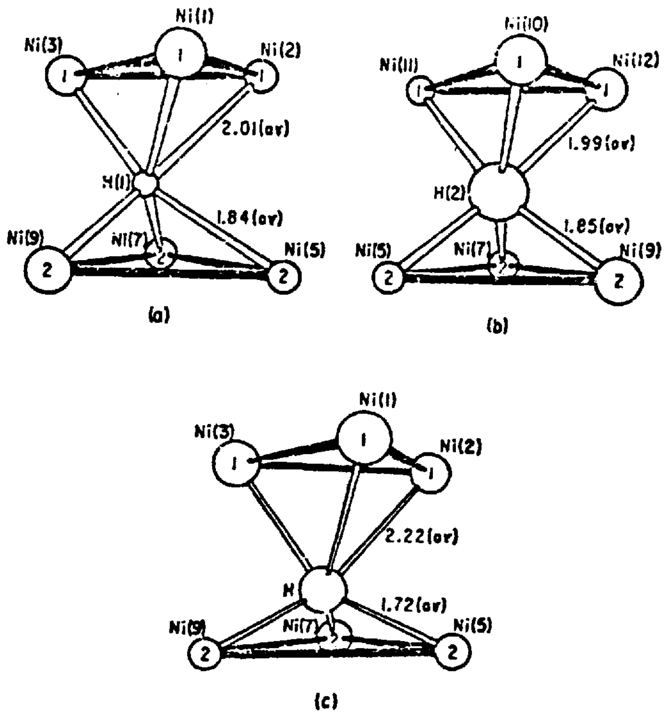

FIGURE 12 Structures of the two analogous Ni_6H fragments (a) and (b) of $[Ni_{12}(H)_2(CO)_{21}]^{2-}$ and of the Ni_6H fragment (c) of $[Ni_{12}H(CO)_{21}]^-$. (Corresponding to Fig. 7, p. 105 in R. W. Broach, L. F. Dahl, G. Longoni, P. Chini, A. G. Schultz and J. M. Williams, Adv. Chem. Ser. **167**, 93 (1978).)

modes, A_1 and E, are expected for ν(Ni-H): on the basis of the structural parameters (Eq. (1), see later), the unique band was assigned to the E mode, the A_1 mode being expected at low frequency in the δ(Ni-C-O) zone.[50]

The core of $[Co_6H(CO)_{15}]^-$ compound has a slightly distorted octahedral symmetry with an edge significantly longer than the others and the CO groups associated with this long edge in a quasi-"splayed-out" configuration (Fig. 13). This distortion (from O_h to C_{2v} symmetry) should in principle give rise to a splitting of the T_{1u} ν(Co-H) mode, but an approximate calculation indicates the splitting to be within 10 cm^{-1}: so it was not surprising that the INS spectrum of $[(Co_6H(CO)_{15}][Cs]$ exhibited a unique strong peak at ca. 1056 cm^{-1}, easily assigned to the ν(Co-H) mode[52] (Fig. 14). On the contrary, the ir spectra of K^+ salt both in nujol mull and in CsI or KBr disks showed two strong bands, clearly belonging to ν(Co-H) vibrations, because of the temperature sensitivity and of the deuterium frequency shifting.[50] The spectral analysis was complicated by the band intensity variations and by the appearance of new bands due to hydrogenic modes, when the disks were re-grinded and re-pressed (Fig. 15). The well-known easy deprotonation of the cluster by water or oxigenated solvents was invoked to explain this behavior. An equilibrium, as the following one:

$$[Co_6(\mu_6\text{-}H)(CO)_{15}]^- \rightleftarrows [Co_6(\mu_3\text{-}H)(CO)_{15}]^- \rightleftarrows [Co_6(CO)_{15}]^-$$

$$+ \ (H^+ \text{ substrate})$$

should account for the appearance of the new absorptions, due presumably to HCO_3^-, and for the presence of two well-separated ν(Co-H) vibrations.

The discrepancy between the ir and the INS spectra remained

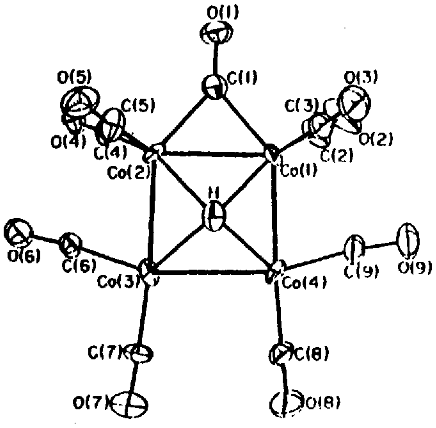

FIGURE 13 A plot of the central equatorial plane of the $[Co_6H(CO)_{15}]^-$ cluster (neutron results). (Corresponding to Fig. 6, p. 1461 in D. W. Hart, R. G. Teller, C. Wei, R. Bau, G. Longoni, S. Campannella, P. Chini and T. F. Koetzle, J. Am. Chem. Soc. **103**, 1458 (1981).)

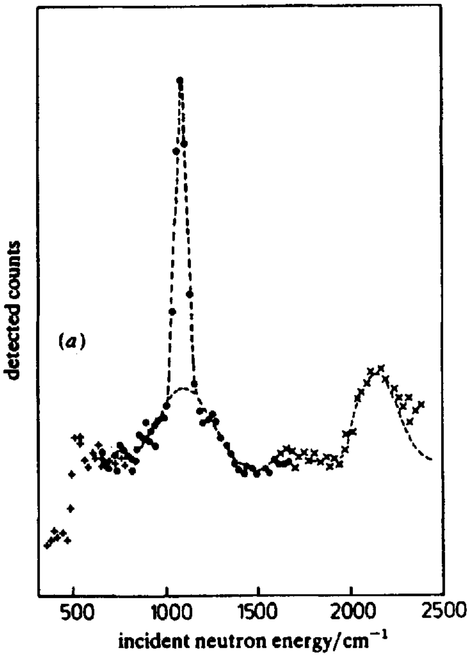

FIGURE 14 INS spectrum of $[Co_6H(CO)_{15}][Cs]$. (Corresponding to Fig. 1(a), p. 1714 in D. Graham, J. Howard, T. C. Waddington and J. Tomkinson, J.Chem. Soc., Faraday Trans. 2 **79**, 1713 (1983).)

unclear, until recent yet unpublished results have shown that just one absorption appears in the ir spectrum of the Cs^+ salt[53] and two peaks appear in the INS spectrum of the K^+ salt.[54] All the data are collected in Table III. At the moment, the most reliable interpretation seems to indicate in the absorption around 1080 cm^{-1} the interstitial hydrogen motion and in the other one, the out-of-cage-bridged hydrogen motion. Nevertheless, the effect of the counter-ions ought to be clarified, as it could be ascribed to their different sizes or to the presence of lattice water in the K^+ salt, as was revealed by the INS spectrum.[54]

The hydrogen which symmetrically bridges an M_3 triangle is not too far from a formal exposed arrangement, so we have included the data on these systems in Table III. If C_{3v} is the local symmetry of an (μ_3-H)M_3 unit, the ν(M-H) vibrations span a symmetric A_1 mode and an asymmetric E mode. The approximate value of the frequency ratio is given by:

$$\nu(A_1)/\nu(E) = \tan \beta/\sqrt{2} \qquad (1)$$

where β is the angle between the M-H vector and the threefold axis.[55] The previous relationship allowed us to assign the M-H bands and, conversely, to calculate the structural parameters from the assignments. The unique result where the H location had been carefully determined by neutron diffraction analysis was encouraging: the β value of the (μ_3-H)Co_3Fe unit is 55.7° (experimental[56]) and 54.7° (calculated[55]).

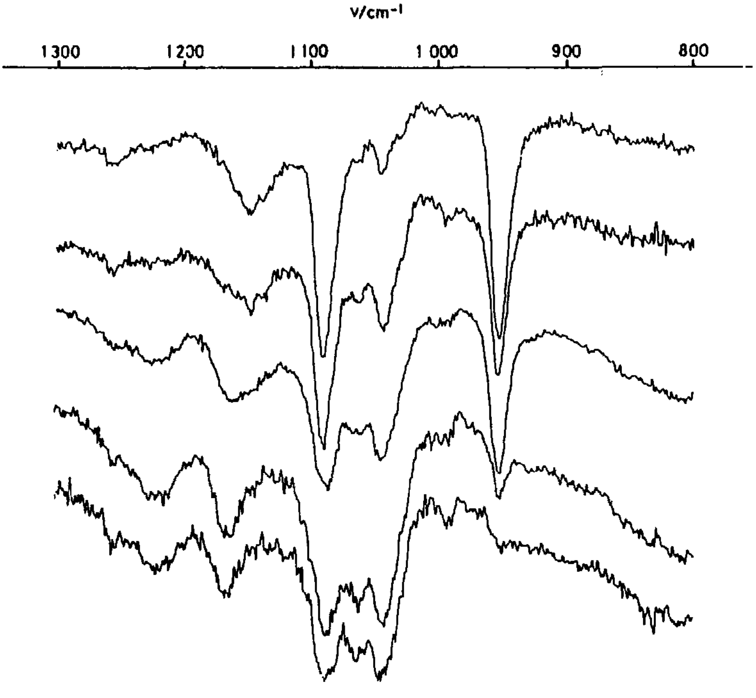

FIGURE 15 Series of subsequent ir spectra of $[Co_6H(CO)_{15}][K]$ at 110 K in CsI disk. (Corresponding to Fig. 2, p. 686 in P. L. Stanghellini and G. Longoni, J. Chem. Soc., Dalton Trans. 685 (1987).)

DISCUSSION

The analysis of the vibrational modes of the X atom was always performed in the approximation that, because X is surrounded by a cage of much heavier metal atoms, the vibrations are likely located on the X atom itself. In other words, the addition of a central atom in a M_n cage increases the number of the vibrational degrees of freedom by three. The "new" modes have essentially ν(M-X) character and transform as x, y and z. In a more correct analysis, not required at this level of approximation, several couplings must be considered, mainly with the δ(M-C-O) modes, very close in energy. On the other hand, the low-frequency normal vibrations, mainly ν(M-M) motions or cage deformations, may have some admixture of a δ(M-X-M) component. The extent of these couplings cannot be measured, unless a complete normal coordinate analysis is performed, which usually is not done because of severe or even insuperable difficulties to assign the normal modes and to calculate a reliable force field.

The three M-X modes are all ir active and give rise to one, two or three bands, depending on the symmetry of the system, which means the symmetry of the metal cage and not that of the whole compound, including the other coordinated ligand. It was pointed out that the band pattern is very sensitive to the geometry of the cage, reflecting even the small changes of the M-M distances[17,21] or the different surroundings in the crystal frame.[30–33] "Mutatis mutandis," the behavior of the band pattern can predict some structural details of unknown cages, like the distortion of the $[Ru_6C(CO)_{16}]^{2-}$ [17] and of $(\mu\text{-}H)_2Os_{10}C(CO)_{24}$ [27] octahedra or the shape of the $Ni_{10}C$[21] and of Ru_5C[33] cores.

An easily achievable model to calculate the force constants seems to be the simple valence force field (SVFF), which uses a complete G matrix and a diagonal F matrix only. The needlessness of the off-diagonal matrix elements, i.e., the interaction force constants, to describe the force field means that the interaction between the interstitial atom and the metal atoms of the cage can be better described as a delocalized bond between the MO's of the cage and the X atomic orbitals, than as a strongly localized direct bond between X and a single M. Two examples were reported, where this bonding picture suggests a force field suitable to a good fit between observed and calculated frequencies. In the $[M_6X(CO)_{15}]^{n-}$ (M = Co, Rh; X = C, n = 2; X = N, n = 1), two different interactions were suggested for X to bond rectangular and triangular faces of the cage.[28] In the capped Re carbido octahedra the two interactions concern the capped and the non-capped octahedral faces, the former being lower because the capping atom removes the MO density from the Re_3 triangle, so decreasing the overlap with the carbon p_z.[21] As a consequence, two force constants are required, one concerning the motion of the X atom along the main symmetry axis (f_z), the other one, related to the vibration on the transversal plane (f_{xy}): in both cases, the relation $f_{xy} > f_z$ holds.

The question is: how reliable are the fc values calculated in this way? In principle, in the absence of any detailed NCA, the reliability ought to be poor. Nevertheless, it is commonly accepted that, when a group of atoms in a molecule is only weakly coupled to the remainder, it may be treated separately in order to calculate approximate force constants.[57] This seems to be the case here: so the fc values can be considered a rough estimate of the "true" force constants, their acceptability being greater if they are taken into account only as relative values in a homogeneous series. On the other hand, the level of approximation can be indirectly evaluated by comparing the observed values of the frequencies with those calculated by a simplified force field and/or on the ^{13}C, ^{15}N or D isotopomers. Generally, the agreement is acceptable, except for the modes whose frequencies are very close to those of the δ(M-C-O) modes, i.e., near 600 cm^{-1} or below, as the selected examples reported in Table IV can show.

Empirical relationships between the force constant related to the stretch of a bond and the length of the bond itself have often been proposed.[58] The carbido systems offer a set of data large enough to attempt a rationalization, provided that the carbon covalent radius r_C is used, in order to neglect the effect of the metal size on the M-C distance. The average values of r_C, calculated as equal to $d_{M\text{-}C}(av) - (\frac{1}{2})d_{M\text{-}M}(av)$, are plotted in Fig. 16 vs the average values of the force constants.[59]

The uncertainty of the ν(M-C) assignment for M_5C clusters does not allow the calculation of reliable force constants. Nevertheless, as the average frequency of the E mode, whichever the assignment

TABLE IV

Observed (calculated) frequency values (cm^{-1}) for ν(M-X) vibrations

		ν(M-X)	
Complex[a]	Mode	X = $^{12}C/^{14}N$	X = $^{13}C/^{15}N$
$[Ru_6C(CO)_{16}][TMA]_2$	E	719	692(691)
	A	690	662(663)
$Ru_6C(CO)_{17}$	T_{1u}	838	804(805)
$[Re_8C(CO)_{24}][TEA]_2$	E_u	696(696)	670(669)
	A_{2u}	655(654)	637(629)
$[Re_7C(CO)_{21}][TEA]_3$	E	688(689)	662(662)
	A_1	662(662)	640(636)
$[Re_7C(CO)_{22}][TEA]$	A'	695(698)	
	A''	685(682)	
$Co_6C(CO)_{12}(\mu_3\text{-}S)_2$	A_2''	819	790(787)
	E'	548(610)	536(589)
$[Co_6C(CO)_{15}][PPN]_2$	A_2''	772	745(742)
	E'	719	692(691)
$[Rh_6C(CO)_{15}][K]_2$	A_2''	689	664(662)
	E'	653	631(627)
$[Ni_8C(CO)_{16}][TMA]_2$	E	580(579)	557(556)
	B_2	524(529)	
$[Ni_9C(CO)_{17}][TMA]_2$	E	582(581)	560(558)
	A_1	522(523)	506(503)
$[Fe_4C(CO)_{12}][PPN]_2$	B_2	929(931)	896(898)
	A_1	666(673)	652(650)
	B_1	608(590)	601(572)
$[Fe_4C(\mu\text{-}H)(CO)_{12}][PPN]$	B_2	922(923)	889(891)
	A_1	661(665)	648(643)
	B_1		600(573)
$Fe_4C(CO)_{13}$	B_2	928(930)	895(897)
	A_1	658(667)	645(645)
$[Co_6N(CO)_{15}][TPP]$	A_2''	722	700(698)
	E'	698	678(674)
$[Rh_6N(CO)_{15}][TPP]$	A_2''	645	627(623)
	E'	622	605(601)
$Ru_4N(CO)_{12}(\mu\text{-}H)$	A_1	685(693)	
$Ru_4N(CO)_{12}(\mu\text{-}NCO)$	A_1	595(634)	
$Ru_4N(CO)_{12}(\mu\text{-}NO)$	A_1	591(576)	

[a] For the abbreviations, see Tables I–III.

is, does not vary too much, approximate f_{xv} values have been calculated and reported in the figure.

All the force constant values are collected in Table V. To provide a direct structure/force constant comparison, Table V reports the average $d_{M\text{-}X}$ and r_X values.

Arguing any general rule from the plot could be pretentious, owing to the large spreading of the experimental values, due to the approximation on calculating the force constants. Anyway, if one takes into account the interstitial clusters only, a rough trend might be evidenced, that is, the increase of r_C is suggestive of an increase of the dimension of the cavity where C is located and, consequently, of a decrease of its interaction with the metal cage. As far as the exposed clusters are concerned, the inverse fc/r_C relationship does not hold anymore. Nevertheless, the plots of f_w of Fe_4C clusters and of f_{xy} of M_5C clusters are close to the trend of the interstitials, probably because they are referred to motions which maintain the C atom in the cluster, so resembling the motion of an interstitial atom in a cage. On the contrary, the motion of the exposed C in directions which bring it out of the cluster is

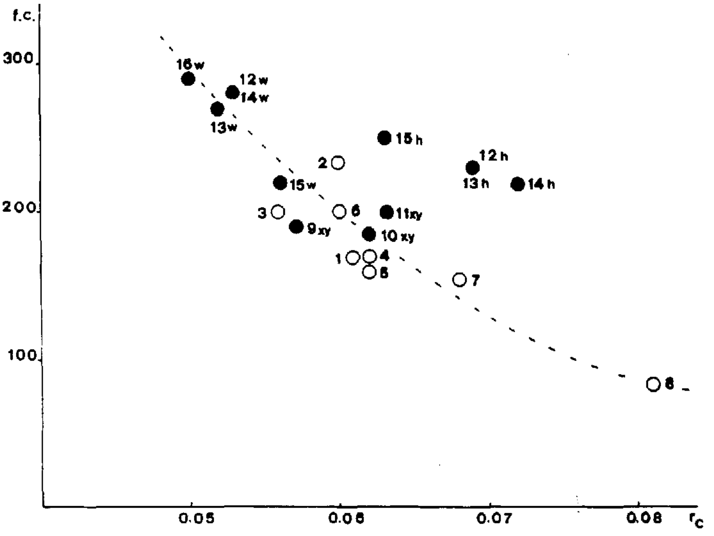

FIGURE 16 Plots of the force constant values related to the M-C stretching vs. the apparent radius of the carbon atom; open circles, interstitial clusters; closed circles, exposed clusters. (1) $[Ru_6C(CO)_{16}]^{2-}$; (2) $Ru_6C(CO)_{17}$; (3) $[Fe_6C(CO)_{16}]^{2}$ (4) $[Re_6C(CO)_{18}(\mu\text{-}H)_2]^{2-}$; (5) $[Re_8C(CO)_{24}]^{2-}$, $[Re_7AgC(CO)_{21}]^{2-}$, $[Re_7C(CO)_{21}]^{3-}$; (6) $[Os_{10}C(CO)_{24}]^{2-}$; (7) $Co_6C(CO)_{12}(\mu_3\text{-}S)_2$; (8) $[Ni_8C(CO)_{16}]^{2-}$, $[Ni_9C(CO)_{17}]^{2-}$; (9) $Fe_5C(CO)_{15}$; (10) $Ru_5C(CO)_{15}$; (11) $Os_5C(CO)_{15}$; (12) $[Fe_4C(CO)_{12}]^{2-}$; (13) $[Fe_4C(\mu\text{-}H)(CO)_{12}]^{\delta-}$; (14) $Fe_4C(CO)_{13}$; (15) $Fe_4(CH)(\mu\text{-}H)(CO)_{12}$; (16) $[Fe_3RhC(CO)_{12}]^-$ (for *w*, *h*, *xy* symbols, see Table V).

TABLE V

Force constants (Nm^{-1}) and structural parameters (nm) of interstitial and exposed clusters

Complex[a]	fc[b]	$d^{c}_{M\text{-}X}$	r^{c}_{X}	Ref.[d]
$[Ru_6C(CO)_{16}][TMA]_2$	168	0.205	0.061	18
$Ru_6C(CO)_{17}$	234	0.205	0.060	16
$[Fe_6C(CO)_{16}][TMA]_2$	200	0.189	0.056	19
$[Re_6C(CO)_{18}(\mu\text{-}H)_2][TEA]_2$	170	0.214	0.062	20
$[Re_8C(CO)_{24}][TEA]_2$	150 *z*	0.212	0.062	23
	170 *xy*			
$[Re_7AgC(CO)_{21}][TEA]_2$	145 *z*	0.213	0.062	24
	160 *xy*			
$[Re_7C(CO)_{21}][TEA]_3$	160 *z*	0.212	0.062	25
	170 *xy*			
$[Os_{10}C(CO)_{24}][TMA]_2$	200	0.204	0.060	26
$Co_6C(CO)_{12}(\mu_3\text{-}S)_2$	155	0.194	0.068	15
$[Co_6C(CO)_{15}][PPN]_2$	204 *z*	0.195	0.068	60
	235 *xy*			
$[Rh_6C(CO)_{15}][K]_2$	209 *z*	0.213	0.073	61
	261 *xy*			
$[Ni_8C(CO)_{16}][TMA]_2$	84	0.209	0.081	29
$[Ni_9C(CO)_{17}][TMA]_2$	84	0.209	0.081	29
$Fe_5C(CO)_{15}$	ca. 190 *xy*	0.189 *xy*	0.057 *xy*	13
$Ru_5C(CO)_{15}$	ca. 185 *xy*	0.204 *xy*	0.062 *xy*	62
$Os_5C(CO)_{15}$	ca. 200 *xy*	0.206 *xy*	0.063 *xy*	63
$[Fe_4C(CO)_{12}][PPN]_2$	280 *w*	0.180 *w*	0.053 *w*	64
	230 *h*	0.196 *h*	0.069 *h*	
$[Fe_4C(\mu\text{-}H)(CO)_{12}][PPN]$	270 *w*	0.179 *w*	0.052 *w*	65
	230 *h*	0.199 *h*	0.069 *h*	

$Fe_4C(CO)_{13}$	280 *w*	0.180 *w*	0.053 *w*	66
	220 *h*	0.199 *h*	0.072 *h*	
$Fe_4(CH)(\mu\text{-}H)(CO)_{12}$	220 *w*	0.183 *w*	0.056 *w*	67
	250 *h*	0.194 *h*	0.063 *h*	
$[Fe_3RhC(CO)_{12}][PPN]$	290 *w*	0.177 *w*	0.050 *w*	68
$[Fe_3WC(CO)_{13}][PPN]_2$	260 *w*			
$[Co_6N(CO)_{15}][TPP]$	209 *z*	0.194	0.067	2
	261 *xy*			
$[Rh_6N(CO)_{15}][TPP]$	167 *z*			
	207 *xy*			
$Fe_5N(\mu\text{-}H)(CO)_{14}$	290 *z*	0.191 *z*	0.062 *z*	39
	320 *xy*	0.184 *xy*	0.055 *xy*	
$Ru_4N(CO)_{12}(\mu\text{-}H)$	285 *w*	0.193 *w*	0.053 *w*	69
	315 *h*	0.211 *h*	0.071 *h*	
$Ru_4N(CO)_{12}(\mu\text{-}NCO)$	290 *w*	0.190 *w*	0.049 *w*	70
	325 *h*	0.213 *h*	0.072 *h*	
$Ru_4N(CO)_{12}(\mu\text{-}NO)$	290 *w*	0.190 *w*	0.049 *w*	70
	315 *h*	0.216 *h*	0.075 *h*	
$Ru_4N(CO)_{11}(\mu\text{-}H)_3$	240 *w*	0.196 *w*	0.056 *w*	71
	310 *h*	0.206 *h*	0.066 *h*	

---

[a] For the abbreviations, see Tables I–III.

[b] *z* indicates the main symmetry axis; *xy*, the transversal plane; *w*, the wing-tip and *h*, the hinge position of the M_4X butterfly.

[c] *z* and *xy* refer to the M(apycal)-X and M(basal)-X distances in the M_5X square pyramid; *w* and *h* refer to the M(wing)-X and M(hinge)-X distances in the M_4X butterfly.

[d] References are related to the structure of the cluster.

probably subject to a stronger restoring force and the corresponding plots appear to have fc values greater than one could expect on the basis of the apparent r_C. This behavior is still clearer in the isostructual series of Ru_4N clusters, where the values of the Ru-N force constants (Table V) are $f_h > f_w$ even if d_h(Ru-N) is greater than d_w(Ru-N).

Finally, the ionic charge of the whole cluster does not seem to have a significant effect either on the frequency or on the force constant values.[72] This could suggest that, even if the MO calculations predict a negative charge on the interstitial carbido atom,[73] the ionic charge should not affect the size of the C charge when the valence electron number of the clusters is the same.

CLUSTER–SURFACE ANALOGY

The impressive growth of the interstitial cluster compounds has focussed attention on structural similarities between such systems and crystallites of binary metal carbido, nitrido or hydrido, as a part of the so-called "cluster–surface analogy."[74] Even if sometimes this analogy might be elusive or overevaluated, the effort to collect and compare the experimental data on the two fields is certainly useful, divergent chemical behavior being as informative as similarities. So more and more often the vibrational behavior of a chemical species coordinated to a metal cluster is offered as a model for analogous structural units on a metal surface: CO,[75,76] H,[77] alkynes,[78] and various hydrocarbon fragments[79] are the commonest reported examples. In this light, we wish to submit to the reader's attention a selection of vibrational data related to the heteroatoms inserted in a metal lattice or embedded on a metal surface. The list in Table VI cannot be regarded as exhaustive; nevertheless its shortness reflects the paucity of the literature data in this field, except for the hydrogen.[80]

The most interesting structural analogy lies between the environment of a heteroatom in an exposed cluster and of the same atom adsorbed on a surface. As an example, structures of triangular (μ_3-X)M_3, butterfly-shaped (μ_4-X)M_4 and square-pyramidal (μ_5-X)M_5 cluster cores are clearly recognized on atoms adsorbed on (111), (110) and (100) planes of a face-centered-cubic metal,

TABLE VI

Vibrational frequencies (cm^{-1}) of the X atom adsorbed on a metal surface or inserted in a metal lattice cavity

System	Symmetry[a]	ν(M-X)	Ref.
C on W(100)	C_{4v}	548	81
C on W(111)	C_{4v} (?)	565	82
N on Cu(111)	C_{4v}	403	83
N on Ni(110)		411	84
H on Ni(100)	C_{4v}	596	86
H on Pd(100)	C_{4v}	485	87
H on Rh(100)	C_{4v}	660 ν_s 1113 ν_{as}	88
H on Ru(001)	C_{3v}	1135 ν_s 821 ν_{as}	89
H on Pt(111)	C_{3v}	550 ν_s 1230 ν_{as}	90
H on Pd(111)	C_{3v}	998 ν_s 773 ν_{as}	91
$VH_{1.92}$	T_d	1131	92
TiH_2	T_d	1202	92
$LaH_{1.94}$	T_d	831	92
$UH_{2.67}$	T_d	903	92
αPdH_x	O_h	460	95
βPdH_x	O_h	549	95
NiH_x	O_h	710	96

[a] Symmetry refers to the local environment of the X atom.

assuming the interaction with metal atoms on the second layer (Fig. 17).

The so-called "β-CO state," i.e., CO adsorbed dissociatively, gives rise to isolated chemisorbed carbido atoms: the loss peak in the EEL spectrum at 68 meV was assigned to the vibration of C in a fourfold site on W(100),[81] whereas the same vibration is not

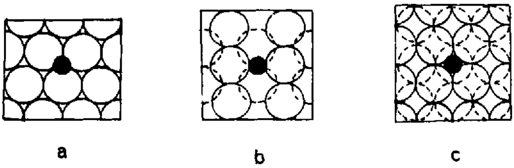

FIGURE 17 Arrangements of heteroatoms adsorbed on (111) face (a), (110) face (b) and (100) face (c) of face-centered-cubic metal crystals (dotted circles indicate the second layer atoms).

resolved from that of the O atom on W(111) and W(110) planes and gives rise to a unique peak at 70 meV.[82]

Adsorption of atomic nitrogen by Cu(111) leads to the formation of a slightly distorted Cu(100)c(2 × 2)N by surface reconstruction, where the nitrogen atoms occupy the four-coordinated sites. The loss peak at 403 cm^{-1} was assigned to copper–nitrogen stretch,[83] similarly to that observed on a nitrided Ni(110) surface at 411 cm^{-1}.[84]

Hydrogen atoms, chemisorbed on metal surfaces are reported to occupy the fourfold site with C_{4v} symmetry or the threefold site with C_{3v} symmetry.[85] In both cases the M-H vibrations belong to a non-degenerate symmetric mode perpendicular to the surface and to a doubly-degenerate asymmetric mode parallel to the surface. Selected assignments are reported in Table VI. For the C_{4v} systems the symmetric mode is located between 500 and 700 cm^{-1}, depending on the coverage and on the kind of crystal used for absorption. The site with C_{3v} symmetry causes two vibrational bands located between 500 and 1250 cm^{-1}, one of which is the dipole-active symmetric mode. The frequency order is $v_s > v_{as}$, but sometimes the reverse, depending on the metal, on the crystallographic plane and, presumably, on the geometry of the adsorbate (Eq. 1).

Interstitial hydrogen in a considerable number of binary hydrides with fluorite structures is located in regular tetrahedral sites. The vibrational frequencies cover a range between 800 and 1350 cm^{-1} and correlate very well with the M-H distance (d), the frequency being proportional to $d^{-3/2}$.[92] Octahedral interstices of the cubic-close-packed metal lattices are known to be occupied by hydrogen atoms in α- and β-phases of palladium–hydrogen systems[93] and in the nickel hydride.[94] All these systems show a sharp peak assigned to the hydrogen motion, along with broad shoulders at higher energy, explained as resulting from the presence of H...H interactions.[95,96] The frequency values are much lower than the previous ones (Table VI), even if d is lower too (2.01 Å for PdH_x, 1.06 Å for NiH_x, 1.9–2.7 Å for tetrahedral hydrides): it was pointed out that in the presence of strong H...H interactions, the simple dependence on d alone does not hold.[95]

The reader can compare Table VI with Tables I–III and draw his own conclusions. To us, any guess seems at the moment inappropriate, failing the factors for a correct comparison, that is, two systems, cluster and surface, with the same metal and the same local environment around the heteroatom. Moreover, a highly CO-covered surface is necessary, because of the presumable effect of neighboring ligands.[97] On the contrary, the two fields have grown until now in different ways and two important gaps are noticeable, on one hand, the exposed hydrido clusters, on the other hand, the spectroscopic data on surface and interstitial binary carbido and nitrido. From the present data it is possible to draw a unique example, where the terms for a comparison are as close as possible: the Ni_{12} interstitial hydrido clusters and the binary nickel–hydride. The similarity of the ν(Ni-H) values could be accidental, nevertheless is encouraging in pursuing the study of the overlap area between the cluster chemistry and the surface chemistry.

Acknowledgments

A NATO grant (P.L.S.) and financial support from the Ministero della Pubblica Istruzione (R.R.) are gratefully acknowledged.

References

1. D. W. Hart, R. G. Teller, C. Wei, R. Bau, G. Longoni, S. Campanella, P. Chini and T. F. Koetzle, Angew. Chem. Int. Ed. **18**, 80 (1979). D. W. Hart, R. G. Teller, C. Wei, R. Bau, G. Longoni, S. Campanella, P. Chini and T. F. Koetzle, J. Am. Chem. Soc. **103**, 1458 (1981).
2. S. Martinengo, G. Ciani, A. Sironi, B. T. Heaton and J. Mason, J. Am. Chem. Soc. **101**, 7095 (1979).
3. K. S. Harpp, C. E. Housecroft, A. L. Rheingold and M. S. Shongwe, J. Chem. Soc., Chem. Commun. 965 (1988).
4. P. Chini, G. Ciani, S. Martinengo, A. Sironi, L. Longhetti and B. T. Heaton, J. Chem. Soc., Chem. Commun. 188 (1979).
5. G. Ciani, L. Garlaschelli, A. Sironi and S. J. Martinengo, Chem. Commun. 563 (1981).
6. K. M. Mackay, B. K. Nicholson, W. T. Robinson and A. W. Sims, J. Chem. Soc., Chem. Commun. 1276 (1984).
7. J. L. Vidal, Inorg. Chem. **20**, 243 (1981).
8. J. L. Vidal and J. M. Troup, J. Organomet. Chem. **213**, 351 (1981).
9. A. Ceriotti, A. Fait, G. Longoni, G. Piro, L. Resconi, F. Demartin, M. Manassero, N. Masciocchi and M. Sansoni, J. Am. Chem. Soc. **108**, 5370 (1986). A. Ceriotti, F. Demartin, G. Longoni, M. Manassero, M. Marchionna, G. Piva and M. Sansoni, Angew. Chem. Int. Ed. **24**, 697 (1985).

10. P. F. Jackson, B. F. G. Johnson, J. Lewis, M. McPartlin and W. J. H. Nelson, J. Chem. Soc., Chem. Commun. 49 (1982).
11. A. Ceriotti, G. Longoni, M. Manassero, N. Maciocchi, L. Resconi and M. Sansoni, J. Chem. Soc., Chem. Commun. 181 (1985).
12. G. Gervasio, R. Rossetti, P. L. Stanghellini and G. Bor, Inorg. Chem. **23**, 2073 (1984).
13. E. H. Braye, L. F. Dahl, W. Hubel and D. L. Wampler, J. Am. Chem. Soc. **84**, 4633 (1962).
14. M. Tachikawa and E. L. Muetterties, Prog. Inorg. Chem. **28**, 203 (1981). J. S. Bradley, Adv. Organometall. Chem. **22**, 1 (1983).
15. G. Bor and P. L. Stanghellini, J. Chem. Soc. Chem. Commun. 886 (1979). G. Bor, U. K. Dietler, P. L. Stanghellini, G. Gervasio, R. Rossetti, G. Sbrignadello and G. A. Battiston, J. Organomet. Chem. **213**, 277 (1981).
16. A. Sirigu, M. Bianchi and E. Benedetti, J. Chem. Soc., Chem. Commun. 596 (1969).
17. P. L. Stanghellini, L. Cognolato, G. Bor and S. F. A. Kettle, Crystallogr. Spectrosc. Res., **13**, 127 (1983).
18. J. S. Bradley, G. B. Ansel and E. W. Hill, J. Organomet. Chem. **184**, C33 (1980).
19. M. R. Churchill and J. Wormald, J. Chem. Soc., Dalton Trans. 2410 (1974).
20. G. Ciani, G. D'Alfonso, P. Romiti, A. Sironi and M. Freni, J. Organomet. Chem. **244**, C27 (1983).
21. P. L. Stanghellini, R. Rossetti, G. D'Alfonso and G. Longoni, Inorg. Chem. **26**, 2769 (1987).
22. T. Beringhelli, G. D'Alfonso, M. De Angelis, G. Ciani and A. Sironi, J. Organomet. Chem. **322**, C21 (1987).
23. G. Ciani, G. D'Alfonso, M. Freni, P. Romiti and A. Sironi, J. Chem. Soc., Chem. Commun. 705 (1982).
24. T. Beringhelli, G. D'Alfonso, M. Freni, G. Ciani and A. Sironi, J. Organomet. Chem. **295**, C7 (1985).
25. G. Ciani, G. D'Alfonso, M. Freni, P. Romiti and A. Sironi, J. Chem. Soc., Chem. Commun. 339 (1982).
26. P. F. Jackson, B. F. G. Johnson, J. Lewis, M. McPartlin and W. J. H. Nelson, J. Chem. Soc., Chem. Commun. 224 (1980).
27. I. A. Oxton, S. F. A. Kettle, P. F. Jackson, F. B. G. Johnson and J. Lewis, J. Mol. Struct. **71**, 117 (1981).
28. J. A. Creighton, R. Della Pergola, B. T. Heaton, S. Martinengo, L. Strona and D. A. Willis, J. Chem. Soc., Chem. Commun. 864 (1982).
29. A. Ceriotti, G. Longoni, M. Manassero, M. Perego and M. Sansoni, Inorg. Chem. **24**, 117 (1985).
30. I. A. Oxton, D. B. Powell, R. J. Goudsmit, B. F. G. Johnson, J. Lewis, W. J. H. Nelson, J. N. Nicholls, M. J. Rosales, M. D. Vargas and K. H. Withmire, Inorg. Chim. Acta Lett. **64**, L259 (1982).
31. A. Gourdon and Y. Jeannin, J. Organomet. Chem. **290**, 199 (1985).
32. I. A. Oxton, D. B. Powell, D. H. Farrar, B. F. G. Johnson, J. Lewis and J. N. Nicholls, Inorg. Chem. **20**, 4302 (1981).
33. C. E. Anson, D. B. Powell, A. G. Cowie, B. F. G. Johnson, J. Lewis, W. J. H. Nelson, J. N. Nicholls and D. A. Welch, J. Mol. Struct. **159**, 11 (1987).
34. P. L. Stanghellini, M. J. Sailor, P. Kuznesof, K. H. Withmire, J. A. Hriljac, J. W. Kolis, Y. Zheng and D. F. Shriver, Inorg. Chem. **26**, 2950 (1987).
35. M. D. Brice and B. R. Penfold, Inorg. Chem. **11**, 1381 (1972).

36. P. L. Stanghellini, L. Cognolato, R. Rossetti and G. Bor, XXII ICCC Budapest 780 (1982).
37. W. L. Gladfelter, Adv. Organomet. Chem. **24**, 41 (1985).
38. The sample was kindly donated by the late Prof. E. L. Muetterties.
39. M. Tachikawa, J. Stein, E. L. Muetterties, R. G. Teller, M. A. Beno, E. Gebert and J. M. Williams, J. Am. Chem. Soc. **102**, 6648 (1980).
40. M. W. Howard, U. A. Jayasooriya, S. F. A. Kettle, D. B. Powell and N. Sheppard, J. Chem. Soc., Chem. Commun. 18 (1979).
41. C. E. Anson, J. P. Attard, B. F. G. Johnson, J. Lewis, J. M. Mace and D. B. Powell, J. Chem. Soc., Chem. Commun. (1986).
42. M_w and M_h stay for metals occupying the wing-tip and the hinge position of the butterfly, respectively.
43. For sake of clarity, the same choice of coordinates was adopted for carbido[34] and nitrido[41] butterfly clusters, so B_1 and B_2 in Ref. 41 become B_2 and B_1, respectively.
44. The $A_1(1)$ mode was not detected.
45. The splitting of several metal-nitrido bands into two or three components was ascribed to the presence of inequivalent molecules in the crystal, rather than to factor-group splitting.[41]
46. P. F. Jackson, B. F. G. Johnson, J. Lewis, P. R. Raithby, M. McPartlin, W. J. H. Nelson, K. D. Rouse, J. Allison and S. A. Mason, J. Chem. Soc., Chem. Commun. 295 (1980).
47. A. N. Fitch, S. A. Barrett, B. E. F. Fender and A. Simon, J. Chem. Soc., Dalton Trans. 501 (1984).
48. R. W. Broach, L. F. Dahl, G. Longoni, P. Chini, A. G. Schultz and J. M. Williams, Adv. Chem. Ser. **167**, 93 (1978).
49. Literature reports several other examples in which the presence of interstitial hydrogen in octahedral, square pyramidal or tetrahedral cavities was indirectly inferred or suggested on the basis of x-ray analysis, nmr spectra or chemical behavior: see Ref. 50 and references cited therein.
50. P. L. Stanghellini and G. Longoni, J. Chem. Soc., Dalton Trans. 685 (1987).
51. I. A. Oxton, S. F. A. Kettle, P. F. Jackson, B. F. G. Johnson and J. Lewis, J. Chem. Soc., Chem. Commun. 687 (1979).
52. D. Graham, J. Howard, T. C. Waddington and J. Tomkinson, J. Chem. Soc., Faraday Trans. 2 **79**, 1713 (1983).
53. P. L. Stanghellini and G. Longoni, unpublished results.
54. A. Albinati, private communication.
55. J. A. Andrews, U. A. Jayasooriya, I. A. Oxton, D. B. Powell, N. Sheppard, P. F. Jackson, B. F. G. Johnson and J. Lewis, Inorg. Chem. **19**, 3033 (1980).
56. R. G. Teller, R. D. Wilson, R. K. McMullan, T. F. Koetzle and R. Bau, J. Am. Chem. Soc. **100**, 3071 (1978).
57. T. G. Spiro, Progr. Inorg. Chem. **11**, 1 (1970). D. F. Shriver and C. B. Cooper, Adv. Infrared Raman Spectrosc. **6**, 127 (1980).
58. P. M. Badger, J. Chem. Phys. **2**, 128 (1934). *Ibid.* **3**, 710 (1935). W. Gordy, ibid. **14**, 305 (1946).
59. Average $d_{\text{M-M}}$ and $d_{\text{M-C}}$ were used owing the uncertainty on bond distances and the slight deformations of the cluster, provided that the values are within a 5% range, otherwise different plots are reported (e.g., Fe_4C clusters). A greater range (±10%) was arbitrarily adopted for the fc values, because of their greater uncertainty.
60. S. Martinengo, D. Strumolo, P. Chini, V. G. Albano and D. Braga, J. Chem. Soc. Dalton Trans. 35 (1985).

61. V. G. Albano, M. Sansoni, P. Chini and S. Martinengo, J. Chem. Soc. Dalton Trans. 651 (1973).
62. D. H. Farrar, P. F. Jackson, B. F. G. Johnson, J. Lewis, J. N. Nicholls and M. McPartlin, J. Chem. Soc., Chem. Commun. 415 (1981).
63. P. F. Jackson, B. F. G. Johnson, J. Lewis, J. N. Nicholls, M. McPartlin and W. J. H. Nelson, J. Chem. Soc., Chem. Commun. 564 (1980).
64. R. F. Boehme and P. Coppens, Acta Cristallogr., Sect. B: Struct. Crystallogr. Cryst. Chem. **B37**, 1914 (1981).
65. E. M. Holt, K. H. Whitmire and D. F. Shriver, J. Organomet. Chem. **213**, 125 (1981).
66. J. S. Bradley, G. B. Ansel, M. E. Leonowicz and E. W. Hill, J. Am. Chem. Soc. **103**, 4968 (1981).
67. M. A. Beno, J. M. Williams, M. Tachikawa and E. L. Muetterties, J. Am. Chem. Soc. **102**, 4542 (1980).
68. J. A. Hriljac, P. N. Swepston and D. F. Shriver, Organometallics **4**, 158 (1985).
69. D. Braga, B. F. G. Johnson, J. Lewis, J. M. Mace, M. McPartlin, J. Puga, W. J. H. Nelson, P. R. Raithby and K. H. Whitmire, J. Chem. Soc., Chem. Commun. 1081 (1982).
70. J. P. Attard, B. F. G. Johnson, J. Lewis, J. M. Mace and P. R. Raithby, J. Chem. Soc., Chem. Commun. 1526 (1985).
71. M. A. Collins, B. F. G. Johnson, J. Lewis, J. M. Mace, J. Morris, M. McPartlin, W. J. H. Nelson, J. Puga and P. R. Raithby, J. Chem. Soc., Chem. Commun. 689, 1983.
72. Compare, for example, the homologous series: $[Fe_4C(CO)_{12}]^{2-}$, $[HFe_4C(CO)_{12}]$ and $Fe_4C(CO)_{13}$; $[Os_{10}C(CO)_{24}]^{2-}$ and $H_2Os_{10}C(CO)_{24}$; $[Re_7C(CO)_{21}]^{3-}$, $[Re_7AgC(CO)_{21}]^{2-}$ and $[Re_7C(CO)_{22}]^{-}$.
73. J. F. Halet, D. G. Evans and D. M. P. Mingos, J. Am. Chem. Soc. **110**, 87 (1988).
74. E. L. Muetterties, Bull. Soc. Chim. Belg. **84**, 959 (1975). E. L. Muetterties, Inorg. Chem. **16**, 3381 (1977). E. L. Muetterties, T. N. Rodin, E. Band, C. F. Brucker and W. R. Pretzer, Chem. Rev. **79**, 91 (1979). N. Sheppard *Vibrational Spectroscopy of Adsorbates*, ed. R. F. Willis, Springer Series in Chemical Physics, Vol. 15, p. 165 (Springer-Verlag, Berlin, 1980).
75. N. Sheppard and T. T. Nguyen, *Adv. Infrared Raman Spectrosc.* (Heyden & Sons, London), **5**, 67 (1978).
76. N. Sheppard and J. Erkelens, Appl. Spectrosc. **38**, 471 (1984).
77. U. A. Jayasooriya, M. A. Chesters, M. W. Howard, S. F. A. Kettle, D. B. Powell and N. Sheppard, Surf. Sci. **93**, 526 (1980).
78. C. E. Anson, B. T. Keiller, I. A. Oxton, D. B. Powell and N. Sheppard, J. Chem. Soc. Chem. Commun. 470 (1983). G. Gervasio, R. Rossetti and P. L. Stanghellini, Organometallics **4**, 1612 (1985). M. Rashidi and J. Puddephatt, Organometallics **7**, 1636 (1988).
79. P. Skinner, M. W. Howard, I. A. Oxton, S. F. A. Kettle, D. B. Powell and N. Sheppard, J. Chem. Soc., Faraday Trans. 2 **77**, 1203 (1981). I. A. Oxton, D. B. Powell, N. Sheppard, K. Burgess, B. F. G. Johnson and J. Lewis, J. Chem. Soc., Chem. Commun. 719 (1982). J. Evans and G. S. McNulty, J. Chem. Soc., Dalton Trans. 79 (1984).
80. The frequencies of some expected modes are absent in the list, because the so-called "metal-surface selection rule" favors the detection of the completely symmetric modes in infrared or in electron energy loss (EEL) spectroscopies.[76]
81. H. Froitzheim, H. Ibach and S. S. Lehwald, Surf. Sci. **63**, 56 (1977).
82. C. Backx, R. F. Willis, B. Feuerbach and B. Fitton, Surf. Sci. **68**, 516 (1977).

83. V. Higgs, P. Hollins, M. E. Pemble and J. Pritchard, J. Electron Spectrosc. Relat. Phenom. **39**, 137 (1986).
84. N. D. S. Canning, PhD Thesis University of East Anglia 1983.
85. K. Cristman, Surf. Sci. Reports **9**, 1 (1988).
86. S. Anderson, Chem. Phys. Lett. **55**, 185 (1970). P. A. Karlson, A. S. Martensson, S. Andersson and P. Nordlander, Surf. Sci. **175**, L759 (1986).
87. C. Nyberg and C. G. Tengstal, Solid State Commun. **44**, 251 (1982).
88. L. J. Richter and W. Ho, J. Vac. Sci. Technol. A **5**, 453 (1987).
89. H. Conrad, R. Scala, W. Stenzel and R. Unwin, J. Chem. Phys. **81**, 637 (1984).
90. A. M. Bart, H. Ibach and H. D. Bruchmann, Surf. Sci. **88**, 384 (1979).
91. H. Conrad, M. E. Kordesch, R. Scala and W. Stenzel, J. Electron Spectrosc. Relat. Phenom. **38**, 578 (1986).
92. D. K. Ross, P. F. Martin, W. A. Oates and R. Khoda Bakhsh, Z. Physik. Chem. Neue Folge **114**, 221 (1979).
93. F. A. Lewis, *The Palladium/Hydrogen System* (Academic Press, New York, 1967).
94. E. O. Wollan, J. W. Cable and W. C. Koehler, J. Phys. Chem. Solids **12**, 206 (1959).
95. J. Howard, T. C. Waddington and C. J. Wright, Chem. Phys. Lett. **56**, 258 (1978).
96. J. Eckert, C. F. Majkzrak, L. Passel and W. B. Daniels, Phys. Rew. **29**, 3700 (1984).
97. Cf. the ν(M-H) shift on the binary hydrides due to the H...H interactions at high H-coverages (Ref. 85).